Biochimica et Biophysica Acta, 946 (1988) 235–243
Elsevier

BBA 74252

Effect of stereoconfiguration on ripple phases ($P_{\beta'}$) of dipalmitoylphosphatidylcholine

Joseph A.N. Zasadzinski

Department of Chemical and Nuclear Engineering, University of California, Santa Barbara, CA (U.S.A.)

(Received 10 August 1988)

Key words: Membrane structure; Ripple phase; Stereo chemistry; Dipalmitoylphosphatidylcholine; Liposome

Mixtures of *sn*-1 (D) and *sn*-3 (L) enantiomers of fully hydrated dipalmitoylphosphatidylcholine (DPPC) were studied with differential scanning calorimetry and freeze-fracture microscopy. The pretransition temperature of racemic mixtures of DPPC was 1.8 C° below that of either pure *sn*-1 or *sn*-3 enantiomers, which had similar pretransition temperatures. The main transition temperature of racemic mixtures was also depressed, but to a lesser extent, 0.8 C°. Freeze-fracture images of liposomes of *sn*-1, *sn*-3, and racemic mixtures of DPPC frozen from the $P_{\beta'}$ phase showed well-defined ripples of wavelength 13 nm. Lipid stereoconfiguration had no effect on ripple wavelength, configuration or amplitude, or on the number and nature of surface defects.

Introduction

Saturated phospholipids, notably dimyristoylphosphatidylcholine (DMPC), dipalmitoylphosphatidylcholine (DPPC) and distearoylphosphatidylcholine (DSPC), undergo as many as three distinct, reversible thermal transitions when dispersed in water: a subtransition, pretransition, and main transition as the temperature is raised, separating the phases L_c, $L_{\beta'}$, $P_{\beta'}$ and L_α, respectively [1–3]. The temperatures and enthalpies of these transitions depend on the acyl chain length [4], pressure [5], the phospholipid headgroup [6,7] and the pH and ionic strength of the aqueous phase [8,9].

In excess water (> 30% by weight [10]) the main, or gel–liquid crystalline transition is believed to be caused by the two-diminished melting of the acyl chains of the phospholipids [10,11]. In the L_α phase, the intermolecular order in each half of the bilayer is short-range and liquid-like and the intramolecular *trans–gauche* rotational order of the acyl chains is low [10,11]. The bilayers are smooth and the molecules on average are perpendicular to the bilayer. The symmetry is similar to a Smectic-A.

In the $P_{\beta'}$ phase, the hydrocarbon chains are frozen into a nearly all-*trans* configuration [12], the molecules in each bilayer are packed into a two-dimensional hexagonal lattice with long-range correlations [13,14], and the intralayer self-diffusion coefficient is small [15]. There still exists some disagreement as to whether the molecules are tilted [10] or perpendicular to the bilayer [4]. The bilayers in the $P_{\beta'}$ phases are characterized by regular corrugations, hence the common name of ripple phase X-phase diffraction [3,10,11] and freeze-fracture electron microscopy [13,14,16,17] find the ripple wavelength in excess water to be 12–16 nm. Freeze-fracture images also show re-

Abbreviations: DMPC, dimyristoylphosphatidylcholine; DSPC, distearoylphosphatidylcholine; DSC, differential scanning calorimetry.

Correspondence: J.A.N. Zasadzinski, Department of Chemical and Nuclear Engineering, University of California, Santa Barbara, CA 93106, U.S.A.

0005-2736/88/$03.50 © 1988 Elsevier Science Publishers B.V. (Biomedical Division)

gions of a second ripple shape and wavelength of about 23–25 nm [13,17], although these longer wavelength ripples are not apparent in X-ray diffraction. The structural details of the ripples are still not completely determined. Some theoretical models predict a sinusoidal modulation [10,11,18], while others predict a sawtooth modulation [13,17,19,20]. The reported ripple amplitudes range from 8 [10] to 25 Å [11]. The most direct measurements by scanning tunneling microscopy of freeze-fracture replicas of DMPC show an asymmetric sinusoidal modulation of peak to trough height 4.5 nm and wavelength 12.0 nm [32].

Below the pretransition temperature is the $L_{\beta'}$ phase, characterized by smooth, flat bilayers with the acyl chains fully extended (all-*trans* configuration) and titled with respect to the bilayer normal [2]. This phase is similar to the Smectic-G. The low-temperature $L_{\beta'} \rightarrow L_c$ transition involves a modification of the hydrocarbon chain packing and dehydration of the phosphocholine headgroups [2].

The mechanism of the pretransition is poorly understood. Many theories have suggested that the ripples are caused, at least in part, by the mismatch between the projected area of the hydrocarbon chains and the polar headgroups [15–21]. To accommodate the mismatch, the molecules tilt in the $L_{\beta'}$ phase and ripple in the $P_{\beta'}$ phase. However, it is also well known that the nature of the polar headgroup and its interaction with neighboring molecules and the solvent also influence the pretransition. Removing a single methyl group (or more) from phosphocholine results in the elimination of the ripple phase [7]; saturated phosphatidylethanolamines also do not show a pretransition. Mixtures of *N*-methyldimyristoylphosphatidylethanolamine with DMPC show a pretransition only for DMPC fractions above 85% [13]. Adding salts or ethylene glycol to the aqueous phase also eliminates the pretransition [8,9,22] as does changing the pH [8]. To explain these results, several authors [18,20,23] have suggested that the pretransition involves an order–disorder transition of the lipid headgroups. Further evidence of the role of the headgroup configuration on the pretransition was given by Eklund et al. [6], who showed that the pretransition of a racemic mixture of *sn*-1 and *sn*-3 DMPC occurred approx. 2 C° below that of either the pure *sn*-1 or *sn*-3 enantiomers, McConnell and co-workers [24,33,34] have also shown the influence of stereochemistry on the phase behavior of monolayers of DPPC at the air/water interface. The handedness of solid domains of the monolayer was related to the enantiomorphic configuration of the lipids composing the monolayer. This suggests that the chiral center of the headgroup induces a long-range orientational order within the monolayer.

If this same long-range chiral orientational order were present between the molecules in the bilayers of the $P_{\beta'}$ phase, an order–disorder transition might induce a cholesteric liquid crystal-like arrangement of the headgroups. A regular twist induced by the chiral *sn*-2 carbon of DPPC could define the regular periodicity of the ripple corregations, just as it defines the helical pitch of a typical thermotropic cholesteric [25]. Natural DPPC is purely left-handed (*sn*-3). Neighboring DPPC molecules could rotate around their long axes by a given amount along a direction perpendicular to the ripples.

This rotation might also result in the 'vertical' displacement of the molecules out of the bilayer plane by the following argument. The average displacement of a single DPPC molecule in the ripple phase is on the order of 2.5 Å, or about one or two CH_2 groups per molecule [3,11,32]. This vertical offset is similar to the difference in penetration into the bilayer between acyl chains in symmetric saturated phosphatidylcholines [2,8,26,27]. For any of the saturated phosphatidylcholines, the *sn*-2 acyl chain protrudes sideways from the glycerol axis and bends over at the second carbon, so that the extended length of the chain is two to three carbons shorter than in the *sn*-3 position (*sn*-1 in the enantiomer). The electron density maps of bilayers determined by X-ray diffraction show a lower electron density toward the center of the bilayer that can be ascribed to some space around the methyl end of the phospholipid. While the tilt of the molecules in the gel state can compensate somewhat for the difference in penetration, it is not sufficient to fill the voids [3]. The principle interaction between the molecules in a bilayer is the van der Waals attraction. Because this interaction falls off as r^{-6} with sep-

aration, it can be truncated and treated as a short-range interaction between nearest neighbors [20]. Under the action of the attractive van der Waals forces, the molecules in a bilayer will tend to peak as closely as their geometry allows. To attain the maximum contact between adjacent acyl chains, the molecules might stack with a vertical offset of a CH_2 group because of the difference in penetration depth [11,20]. An alternate explanation for the offset is the headgroup-tailgroup cross-sectional area mismatch, which might prevent close chain packing unless the molecules were offset vertically by 2–3 Å.

This offset, when combined with the rotation induced by a chiral headgroup, could produce a regular rippled modulation of the bilayer. The 'twisting power' of the chiral center (rotation per molecule) determines the wavelength, P, of the ripples; the amplitude of the ripples would be about $PO/2W$, in which W is the width of the DPPC molecule, about 10 Å, and O is the vertical offset, about 2.5 Å. For DPPC, P is about 13 nm, hence the ripple amplitude is about 16 Å and the total bilayer displacement is about 32 Å, well within the limits published in the literature [10,11,32]. Such an order–disorder transition of the molecules would be of low enthalpy and small volume change compared to the main gel–liquid crystalline transition, also in agreement with experimental data [5]. A detailed treatment of a similar model of the ripple phase (without considering the chiral center) is given by Pearce and Scott [20].

If the ripples are simply related to the chiral nature of DPPC, modifying the twisting power by changing the ratio of left handed (*sn*-3) to right handed (*sn*-1) DPPC should alter both the ripple wavelength and amplitude. This effect is observed in thermotropic cholesterics in which the pitch is a sensitive function of enantiomorphic composition [25]. The ripples should disappear entirely for a racemic mixture of *sn*-1 and *sn*-3 DPPC, just as the cholesteric pitch disappears in racemic mixtures [25].

Materials and Methods

sn-1 (D) and *sn*-3 (L) dipalmitoylphosphatidylcholine were purchased from Sigma Chemical Co. (St. Louis, MO) and were used without further purification. Stock solutions of 20 mg/ml *sn*-1 and *sn*-3 DPPC in chloroform were mixed in the appropriate quantities in glass vials to form mixtures of 0–100 mol% *sn*-3 DPPC. The chloroform was removed under vacuum by rotary evaporation at room temperature. A measured quantity of doubly distilled, filtered water was added to the dried DPPC to give a final concentration of 2 wt% lipid. The lipids were dispersed by heating to 50 °C overnight in a water-bath with gentle agitation. Under these conditions, phospholipids are known to form micron-sized, multilamellar liposomes [28].

Differential scanning calorimetry (DSC) was performed using a Perkin-Elmer DSC-4 cooled by a Perkin Elmer Intracooler. Samples of 3 mg lipid with water were placed in stainless steel samples pans with O-ring seals. Endotherms were recorded at a heating rate of 5 C°/min. An average over several cycles was taken. Endotherms were reproducible to ±0.3 °C. The transition temperatures were taken to be the point of maximum deviation from the baseline.

Specimens for electron microscopy were prepared by the method of Fetter and Costello [29]. Small droplets (0.1–0.5 μl) of the lipid/water mixture were sandwiched between two copper planchettes (Balzers BUO-12-056T; Hudson, NH) to form a 10–50 μm thick layer. Previously, the copper planchettes had been etched for 1 s in concentrated nitric acid to remove any contamination and roughen the planchettes surface. The apparatus used for rapid freezing was a modified version of a Balzers Cryojet QFD 020 jet-freeze device. The sample sandwiches were mounted on a Teflon support arm and placed in a temperature-controlled oven located vertically over the jets of the Balzers Cryojet. Sample temperature was adjusted to be in the middle of the range of the $P_{\beta'}$ phase as measured by DSC. Temperature control prior to freezing was better than 0.1 °C. The samples were equilibrated at the appropriate temperature for a few minutes before a solenoid-actuated mechanism opened a Teflon door at the bottom of the oven and dropped the Teflon arm and samples between the opposed jets of the Balzers cryojet. A photodiode switch initiated the high velocity flow of liquid propane, cooled by liquid nitrogen to −180 °C, which impinged on the copper sand-

wich from both sides, to prove a minimum cooling rate of 10000 C°/s. The frozen copper sandwiches were stored under liquid nitrogen until transfer into a spring-loaded 'mousetrap' carrier. The loaded sample carrier was mounted onto the liquid nitrogen-cooled coldfinger in a Balzers 400 freeze-etch device and the vacuum chamber was evacuated to less than 10^{-7} torr. The temperature of the sample carrier and coldfinger were adjusted to $-170°C$ and the spring mecharism was externally actuated, thereby fracturing the samples. The fracture surfaces were immediately replicated by evaporating 1.5 nm of a platinum carbon mixture from an electrode at a 45° angle to the fracture surface, followed by a 15 nm thick film of carbon at normal incidence to increase the mechanical stability of the replica. The samples and replicas were removed from the vacuum chamber and the samples and copper planchettes were dissolved in chromic acid, leaving the platinum-carbon replicas behind. The replicas were washed in a 50% chloroethanol/water mixture, rinsed in doubly distilled water, and collected on formvar-coated 50 mesh gold electron microscope grids (Pelco, Tustin, CA). The replicas were examined in a JEOL 100 CX scanning transmission electron microscope in the conventional transmission mode using 80 kV electrons. Images were recorded on Kodak electron images plates. Shadows (absence of platinum) appear light in the prints.

Ripple periodicities were measured using optical diffraction from the electron microscope negatives [13] using a Polaron optical diffractometer (Polaron, Hatfield, PA). A collimated and filtered helium-neon laser beam was spread to about 1 cm diameter and passed through a selected are of the negative. After passing the beam through a weakly converging lens, the diffraction pattern of the negative was recorded on Polaroid film. Absolute spacings were calculated by comparison to equal magnification TEM images of catalase crystals (Balzers) of known d-spacing. Areas chosen for optical diffraction were from large, planar liposomes with well-aligned ripples. Ripple periodicities were measured only from those areas that exhibited at least two orders of reflection, indicating well-aligned, parallel ripples (see Fig. 3–5). Periodicities were accurate to within ±0.3 nm.

Experimental observations

DSC

The main transition temperatures of *sn*-1 and *sn*-3 DPPC were the same within the experimental accuracy (±0.3°C); 41.6°C for *sn*-3 (L) DPPC and 41.8°C for *sn*-1- (D) DPPC, both in good agreement with published values. The main transition of mixed *sn*-1 and *sn*-3 liposomes showed a systematic depression which depended on the molar proportions of the enantiomers (Fig. 1). The maximum deviation was for a racemic (1 : 1) mixture which had a transition temperature of 41.0°C. Eklund et al. [6] did not observe any depression in the main transition of mixtures of *sn*-1 and *sn*-3 DMPC. The main transitions of all mixtures were sharp and showed no signs of broadening for any compositions, suggesting that the enantiomers formed ideal mixtures. This is at variance with the results of Boyanov et al. [30], who observed a broadening of the main transition of mixtures compared to pure *sn*-3 (or *sn*-1) DPPC. Most likely, these discrepancies are due to differences in sample history or lipid purity.

The pretransition temperatures of pure *sn*-1 and *sn*-3 DPPC were also the same within experimental accuracy: 35.8 and 35.7°C, respectively. These values are in good agreement with those in the literature. The pretransition of mixtures were consistently shifted to lower temperatures and the

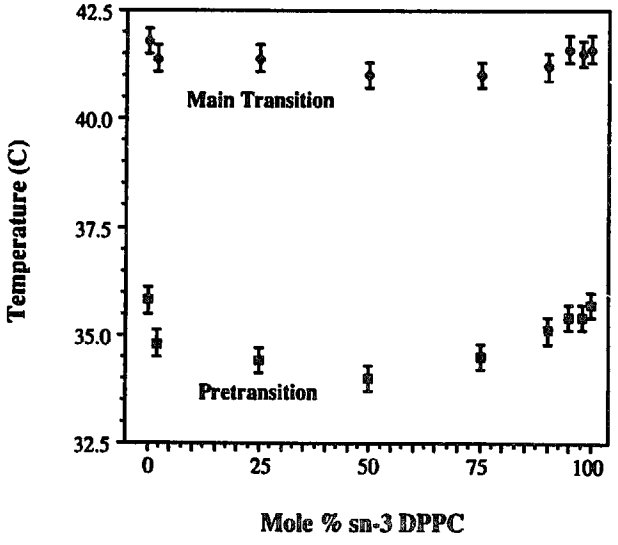

Fig. 1. Endotherm peak temperatures of transitions in mixtures of *sn*-1 and *sn*-3 DPPC.

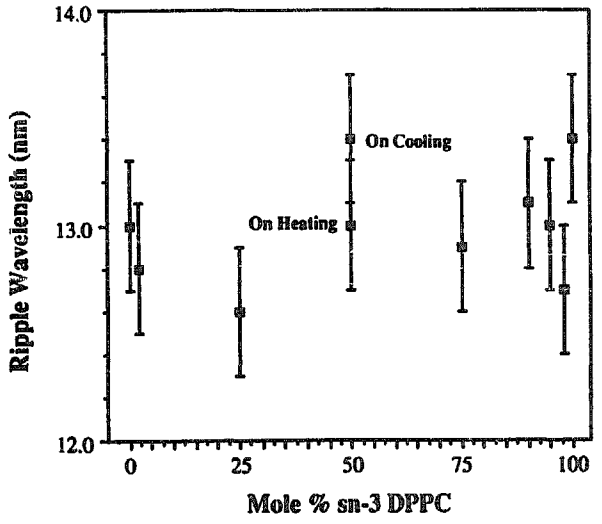

Fig. 2. Ripple wavelength measured by optical diffraction as a function of enantiomer composition. Error in measurement is ±0.3 nm. No significant difference in ripple wavelength with enantiomer fraction was observed.

deviation was largest for a racemic mixture; the pretransition temperature was 34.0°C for a 1:1 mixture of *sn*-1 and *sn*-3 DPPC. This is in agreement with Eklund et al. [6] who observed a 1.8°C depression in the pretransition temperature of racemic mixtures of DMPC compared to pure *sn*-1 or *sn*-3 DMPC.

Freeze-fracture electron microscopy

Liposomes of all mole fractions exhibited characteristic ripple textures when quenched from temperatures between the pre- and main transitions (see Figs. 3–5). The average wavelength of the ripples measured by optical diffraction of micrograph negatives was 13.0 nm. The wavelength and morphology of the ripples was completely independent of the enantiomorphic composition of the liposomes (Fig. 2). Although the measured wavelength varied from 12.6 nm for a 25% *sn*-3/75% *sn*-1 mixture to 13.4 nm for a racemic mixture, these values are within the ±0.3 nm accuracy of the experiment. The racemic mixture also had the same ripple wavelength when brought into the $P_{\beta'}$ phase from either the Lα or the $L_{\beta'}$ phase. No segregation or phase separation was observed in any of the liposomes, confirming DSC evidence that the enantiomers form ideal solid and liquid mixtures. Typical micrographs and diffractograms are shown in Figures 3–5.

Fig. 3 shows an area of well-aligned ripples from a large planar liposome of pure *sn*-3 DPPC. Optical diffraction from the micrograph negative (Fig. 3b) shows three distinct reflections corresponding to a ripple periodicity of 13.0 nm. An optical diffractogram of a catalase crystal (Balzers, Hudson, NH) of identical magnification used for calibration is shown in Fig. 3c: the bright spots correspond to crystalline d-spacings of 6.85 and 8.75 nm. Fig. 3d shows the typical 3-fold symmetry of the ripple directions; in any given liposome, the ripples align along one of three directions separated by 120°. This is a consequence of the hexagonal packing of the DPPC molecules in the $P_{\beta'}$ phase [2,13,14]. The individual ripples are asymmetric, as can be seen from their two distinct textures: thin dark gray lines separated by bands of medium gray (Fig. 3a), and thin white lines separated by bands of medium gray (Fig. 3d) [13,17].

Fig. 4a is of a liposome of a racemic mixture of DPPC quenched from the $P_{\beta'}$ phase. The ripple configuration and defect textures appear identical to both Fig. 3, pure *sn*-3 DPPC, and Fig. 5, pure *sn*-1 DPPC. The ripple wavelength measured from the optical diffractogram (Fig. 4b) is 13.4 nm. Fig. 4c shows a small area of different ripple morphology with wavelength 25.0 nm (arrow). These W-shaped ripples are incommensurate and of larger amplitude than the smaller ripples [13] and might be caused by a packing defect in the ripple organization [17] or by small concentrations of impurities [13]. The large wavelength ripples only appeared when the $P_{\beta'}$ phase was entered from the higher temperature L_α phase.

Fig. 5a shows ripples of pure *sn*-1 DPPC liposomes quenched from the $P_{\beta'}$ phase. The ripples appear to smoothly descend by a bilayer thickness at the arrows; these might be evidence of edge dislocation loops on interior layers. There are significantly more dislocation defects in liposomes when the $P_{\beta'}$ phase is entered from the low temperature $L_{\beta'}$ phase than from the high temperature L_α phase (see Fig. 4). The defect mobility is much higher in the fluid L_α phase and the dislocations can anneal more quickly than in the semi-crystalline $L_{\beta'}$, or $P_{\beta'}$ phases [31]. The ripples also often associate to form large, three-dimensional macro-ripples such as those shown in Fig. 5c [13].

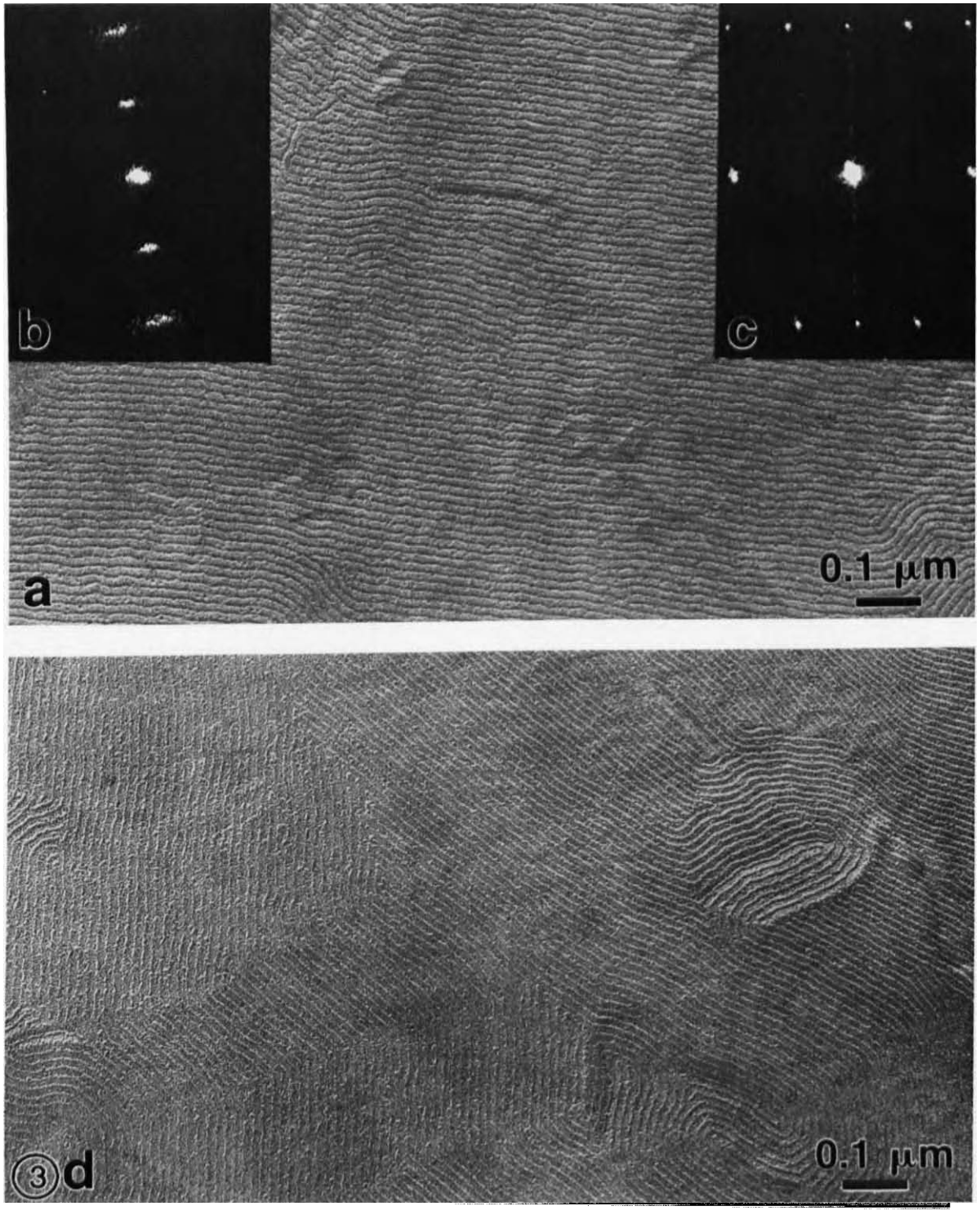

Fig. 3. (a) Freeze-fracture micrograph of pure *sn*-3 DPPC liposome quenched from $P_{\beta'}$ phase exhibiting characteristic ripple texture. (b) Optical diffraction of (a) showing bright reflections corresponding to ripple periodicity of 13 nm. (c) Optical diffraction of catalase calibration sample. Lattice spacings are 6.85 (vertical) and 8.75 nm (horizontal). (d) Freeze-fracture micrograph of pure *sn*-3 DPPC liposome showing typical 3-fold symmetry of ripple direction. Note the reversal of contrast (white lines on gray background) compared to (a), indicating asymmetric ripples.

The macro-ripples are related to the defect topology of the asymmetric ripples in the $P_{\beta'}$ phase, which only allows integer strength disclinations [13,17].

Discussion and Conclusions

If the regular ripples of the $P_{\beta'}$ phase were a result of the chirality of the *sn*-2 carbon of DPPC,

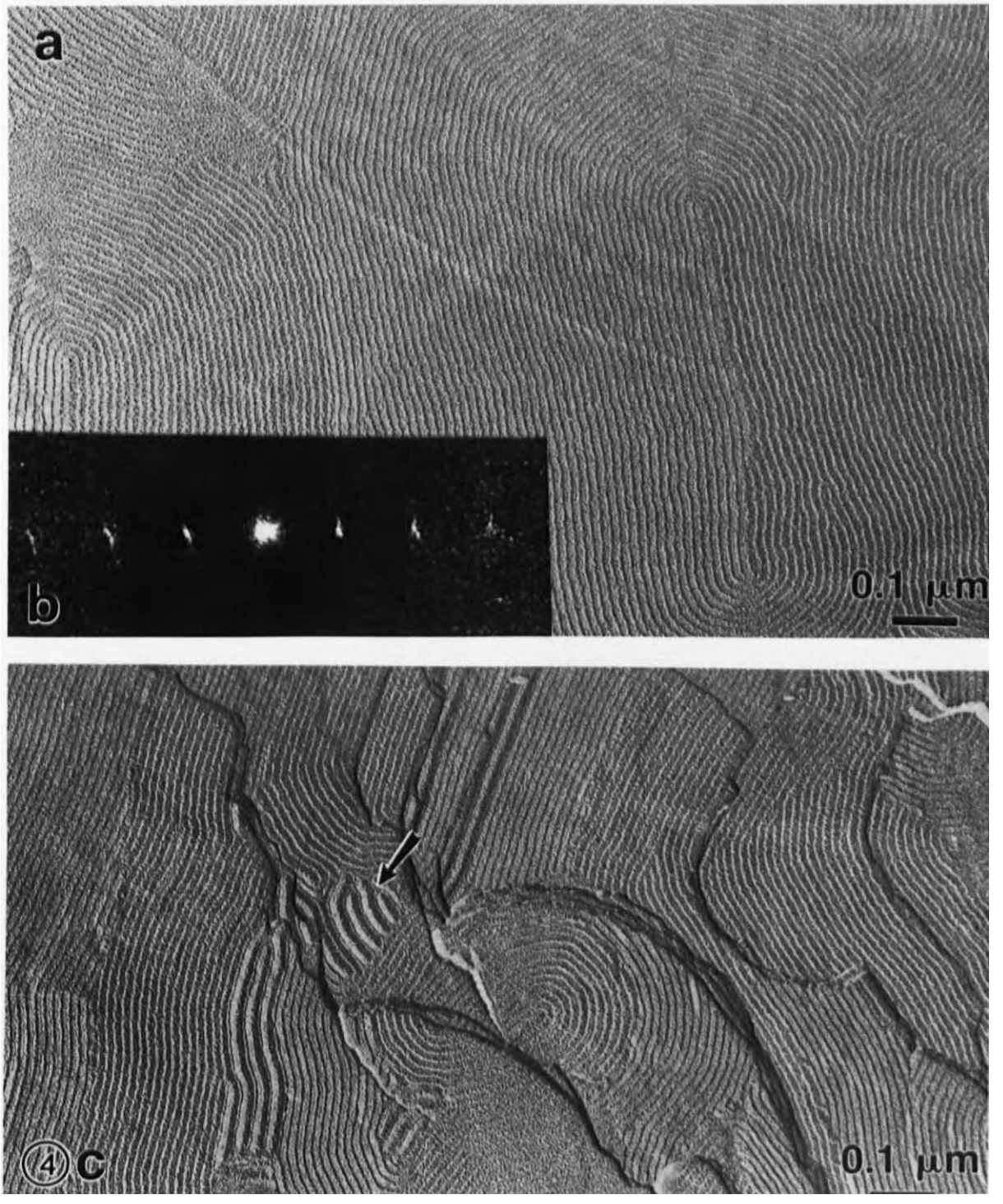

Fig. 4. (a) Racemic mixture of *sn*-1 and *sn*-3 DPPC. No significant different in ripple morphology compared to pure *sn*-1 or *sn*-3. (b) Optical diffraction of (a). (c) Defect texture of ripples showing 3-fold symmetry and small patches of symmetric, longer wavelength ripples at the arrow.

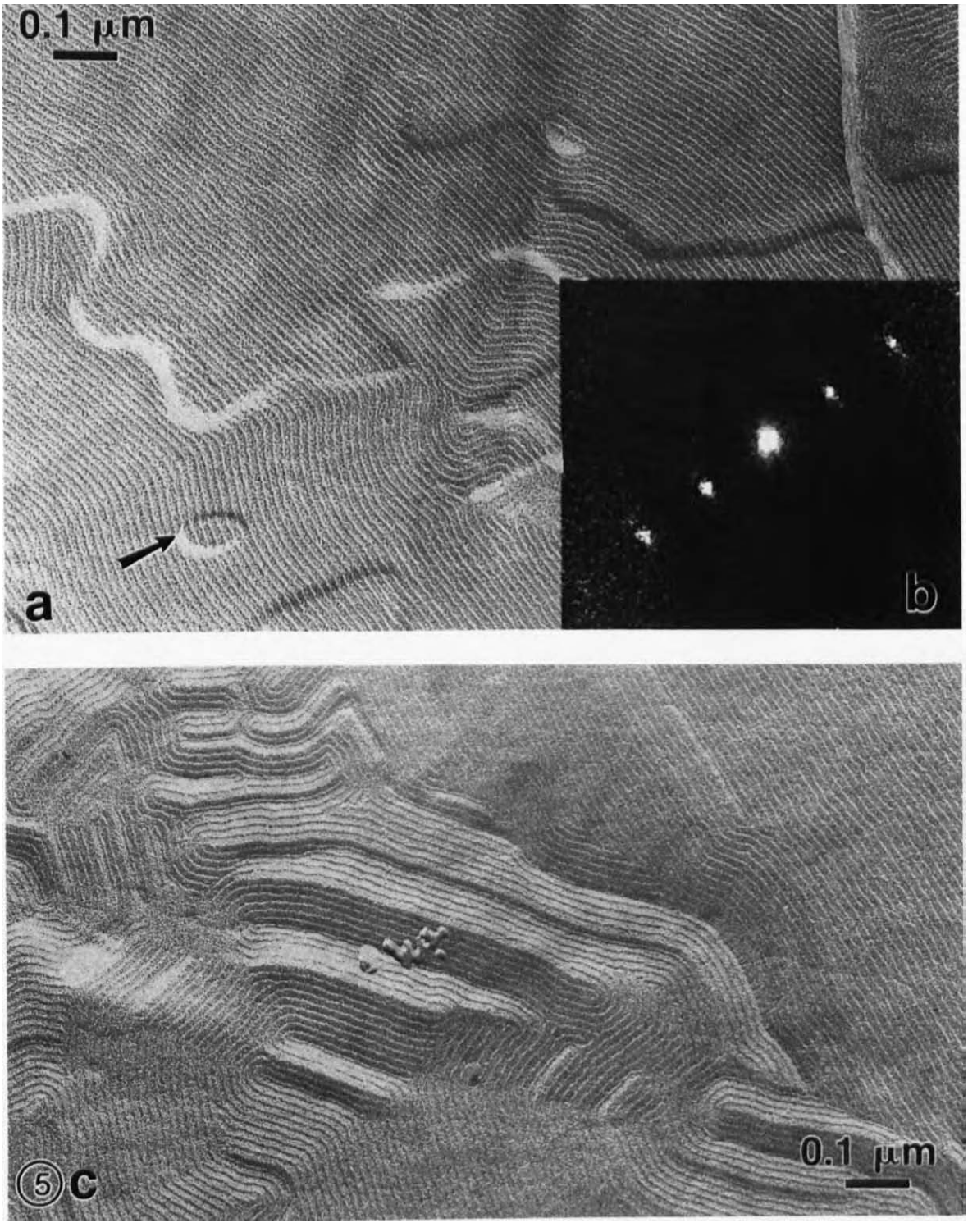

Fig. 5. Pure *sn*-1 DPPC liposome quenched from $P_{\beta'}$ phase. Step traversed by ripples at arrows are indications of edge dislocation loops on underlying layers. (b) Optical diffraction of (a). (c) Three-dimensional macro-ripples caused by defect topology of asymmetric ripples.

the wavelength of the ripples should show a maximum for a racemic mixture and minimums for both pure *sn*-1 and *sn*-3 DPPC. As the wavelength is independent of enantiomorphic composition, the $P_{\beta'}$ phase is not caused by the chirality of DPPC as proposed in the Introduction. However,

the depression of the $L_{\beta'} \rightarrow P_{\beta'}$ transition temperature measured by DSC and the monolayer experiments of McConnell et al. [24] show that chirality does play a part in the transition. The long-range chiral order might exist in the $L_{\beta'}$ phase, giving way to a more disordered structure in the $P_{\beta'}$ phase. The decrease in the transition temperature is more likely to be due to the increased entropy of the racemic mixture relative to its pure enantiomeric components than any specific effects of stereoconfiguration, as suggested by Eklund et al. [6]. The main transition, with a large transition enthalpy, should be less affected by the mixing than the pretransition, which has a much smaller transition enthalpy, as is experimentally observed. Future freeze-fracture experiments on the defect structures in the $L_{\beta'}$ phase, especially on the spiral defects observed by Rüppel and Sackmann [17], should reveal any long-range chiral orientational order. The idea that the vertical displacement of the molecules in the ripple phase is caused by the natural difference in penetration of the acyl chains in symmetric phospholipids might be checked by synthesizing asymmetric lipids to compensate for the unequal penetration [3]. It seems necessary for new theories to include details of the molecular structure of saturated phosphatidylcholines in order to elucidate the nature of the $P_{\beta'}$ phase.

Acknowledgements

I would like to acknowledge the technical help of M.J. Sammon in preparing the freeze-fracture replicas and P. Cladis and P. Finn in preparing the DSC samples. I am grateful to Saul Meiboom for many helpful discussions on the nature of chirality in liquid crystals. The experimental work was done at AT&T Bell Laboratories. Financial support was provided by the donors of the Petroleum Research Fund and by a National Science Foundation Presidential Young Investigator Award No. CBT 86-57444.

References

1 Chen, S.C., Sturtevant, J.M. and Gaffney, B.J. (1980) Proc. Nat. Acad. Sci. USA 77, 5060–5068.
2 Ruocco, M.J. and Shipley, G.G. (1982) Biochim. Biophys. Acta 691, 309–320.
3 Small, D.M. (1986) The Physical Chemistry of Lipids, in Handbook of Lipid Research, Vol. 4 (Hanahan, D.J., ed.), Ch. 12, Plenum Press, New York.
4 Silvius, J.R., Read, B.D. and McElhaney, R.N. (1979) Biochim. Biophys. Acta 555, 175–178.
5 Turley, W.D. and Offen, H.W. (1985) J. Phys. Chem. 89, 39628b13964.
6 Eklund, K.K., Virtanen, J.A. and Kinnunen, P.K.J. (1984) Biochim. Biophys. Acta 793, 310–312.
7 Vaughan, D.J. and Keough, K.M. (1974) FEBS Lett. 47, 158–161.
8 Yeagle, P.L. (1978) Acc. Chem. Res. 9, 321–327.
9 Steim, J.M. (1968) Adv. Chem. Ser. 84, 259–302.
10 Janiak, M.J., Small, D.M. and Shipley, G.G. (1979) J. Biol. Chem. 254, 6068–6078.
11 Stamatoff, J., Feuer, B., Guggenheim, H.J., Tellez, G. and Yamane, T. (1982) Biophys. J. 38, 217–226.
12 Chapman, D. (1972) Ann. NY Acad. Sci. USA 195, 195–212.
13 Zasadzinski, J.A.N. and Schneider, M.B. (1987) J. Phys. (Paris) 48, 2001–2011.
14 Hatta, I., Kato, S. and Ohki, K. (1986) Mol. Cryst. Liq. Cryst, in press.
15 Schneider, M.B., Chan, W.K. and Webb, W.W. (1983) Biophys. J. 43, 157–173.
16 Luna, E.J. and McConnell, H.M. (1977) Biochim. Biophys. Acta 466, 381–392.
17 Ruppel, D. and Sackmann, E. (1983) J. Phys. (Paris) 44, 1025–1034.
18 Doniach, S. (1979) J. Chem. Phys. 70, 4587–4596.
19 Parsegian, V.A. (1983) Biophys. J. 44, 413–415.
20 Pearce, P.A. and Scott, H.L. (1982) J. Chem. Phys. 77, 951–958.
21 Falkovitz, M.S., Seul, M., Frisch, H.L. and McConnell, H.M. (1982) Proc. Nat. Acad. Sci USA 79, 3918–3921.
22 Inoko, Y. and Mitsui, T. (1978) J. Phys. Soc. Jap. 44, 1918–1924.
23 Nagle, J.F. (1973) J. Chem. Phys. 58, 252–264.
24 Weis, R.M. and McConnell, H.M. (1984) Nature 310, 47–49.
25 DeGennes, P.G. (1974) The Physics of Liquid Crystals Ch. 6, Clarendon Press, Oxford.
26 Hauser, H., Pascher, I., Pearson, R.H. and Sundell, S. (1981) Biochim. Biophys. Acta 650, 21–51.
27 Seelig, J. and Seelig, A. (1980) Q. Rev. Biophys. 13, 19–48.
28 Zasadzinski, J.A.N., Scriven, L.E. and H.T. Davis (1985) Phil. Mag. A. 51, 287–302.
29 Fetter, R.D. and Costello, M.J. (1986) J. Microsc. (London) 141, 277–290.
30 Boyanov, A.I., Tenchov, B.G., Koynova, R.D. and Kovmanov, K.S. (1983) Biochim. Biophys. Acta 732, 711–713.
31 Chan, W.K. and Webb, W.W. (1981) J. Phys. (Paris) 42, 1007–1013.
32 Zasadzinski, J.A.N., Schneir, J., Gurley, J., Elings, V. and Hansma. P.K. (1988) Science 239, 1014–1015.
33 McConnell, H.M., Keller, D. and Gaub, H.E. (1986) J. Phys. Chem. 90, 1717–1721.
34 Gaub, H.E., Moy, V.T. and McConnell, H.M. (1986) J. Phys. Chem. 90, 1721–1725.